Int J Environ Res (2022) 16:77
https://doi.org/10.1007/s41742-022-00448-z

RESEARCH PAPER

Vertical Distribution of Phosphorous Fractions and Bioavailability of the Nutrient in the Southern Indian Ocean

Muhammed Nayeem Mullungal[1] · Sruthi Thalayappil[2] · Sajna Peediyakkathodi[3] · Palliparambil Michael Salas[4] · Chenicherry House Sujatha[4] · Chelakkal Sukumaran Ratheesh Kumar[3]

Received: 4 April 2022 / Revised: 13 July 2022 / Accepted: 26 July 2022 / Published online: 24 August 2022

Abstract

The study evaluated concentration, vertical distribution, and bioavailability of phosphorus fractions in the Indian Ocean core sediments. Sediment samples were collected from two sites in the Indian Ocean during January–February 2010 using gravity corer. Phosphorus fractions in sediments were analyzed by a modified sequential extraction procedure (SEDEX). The vertical profile revealed silt and clay as dominant grain size fractions in both cores. The enriched levels of organic carbon were observed in samples due to adsorption on fine grained sediments. Loosely bound P was the most dominant fraction, and its higher concentration in sediments was due to increased productivity and subsequent inputs of biogenic components. Detritus from marine organisms and lower oxygen concentrations (depleted E^h values) enhanced the production of authigenic P. The lower iron bound P fraction at specific depths was attributed to the nature of Fe minerals present within sediments. Decreased level of organic phosphate fraction was due to mineralization. The presence of Detrital P, the diagenetically stable form of P, might be due to inputs from the Himalayan, peninsular Indian, and Sri Lankan regions. The biogenic form was the dominant phosphate fraction throughout the cores suggesting the dissolution of fish debris. Estimated bioavailable phosphorous (BAP) ranged from 82.2 to 98.7% in Core I and from 90.21 to 92.98% in Core II, suggesting the fact that a major portion of the phosphate was bioavailable and hence the alterations in environmental conditions can release the BAP to water column resulting in nutrient enrichment.

✉ Muhammed Nayeem Mullungal
mmullungal@qu.edu.qa

[1] Environmental Sciences Program, Department of Biological and Environmental Sciences, College of Arts and Science, Qatar University, Doha, 2713, Qatar

[2] Kerala University of Fisheries and Ocean Studies, Panangad, Kochi, Kerala, India

[3] School of Environmental Studies, Cochin University of Science and Technology, Kochi 682022, Kerala, India

[4] Department of Chemical Oceanography, School of Marine Sciences, Cochin University of Science and Technology, Kochi 682016, Kerala, India

Graphical Abstract

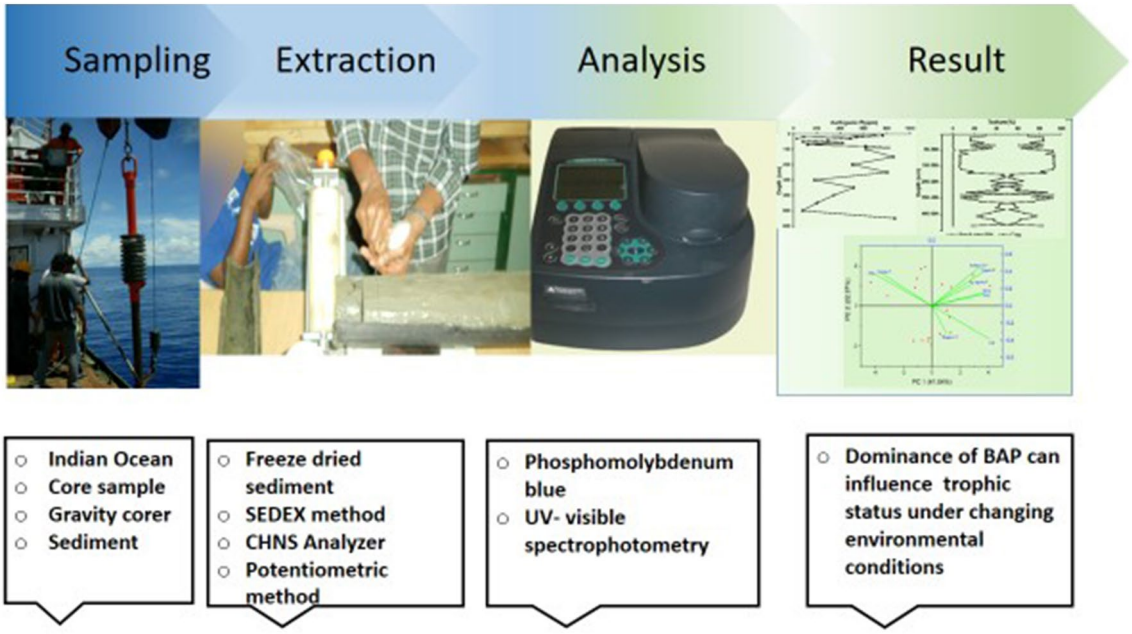

Article Highlights

- **Pioneer study related to nutrient dynamics in the study area.**
- **The contribution of phosphorus from the continental region was established.**
- **Enhanced bioavailable P can lead to a eutrophic state under changing environmental conditions.**

Keywords Phosphorous fractions · Core sediments · SEDEX method · Bioavailability · Indian Ocean

Introduction

Phosphorus (P) serves as a critical factor in regulating biocommunity structure and functions and significantly influences the biogeochemical cycles of other elements in the environment. It is an essential component of several biological molecules (such as ATP, DNA, RNA, protein, enzymes, etc.) and a building block of the cells, cellular elements, bones, teeth, etc. (Tyrrell 1999; Ruttenberg 2003; Reddy et al. 2005; Serna and Bergwitz 2020). Phosphorus occurs primarily as phosphate in deposits of apatite (Ca_5 F $(PO_4)_3$), a mineral found in igneous, sedimentary, and metamorphic rocks; however, approximately 300 additional minerals containing phosphate (PO_4^{3-}) have been described by Jahnke (1992). Oceanic sediment acts as the sink of P (Leote et al. 2014; Abu Hmeidan et al. 2018; Jiang et al. 2018; Dan et al. 2020; Maslukah et al. 2021) as well as a source when dissolved P is low (Jiang et al. 2018; Gurung et al. 2020). Phosphorus is usually released into oceanic and marine waters owing to rock weathering and continental erosion. Phosphorus is discharged into aquatic environments in either dissolved or suspended form by the rivers. Other causes that contribute to increasing phosphorus loadings in the environment include the deposition of suspended particles in the atmosphere, volcanic ash, and inorganic dust (Delaney 1998; Benitez-Nelson 2000; Bagalwa 2021).

Phosphorus is present in the sediments either in bioavailable or non-bioavailable form. "Bioavailable phosphate refers to the sum of immediately available phosphate and phosphate, which can be transformed into a functional form by alterations in environmental conditions and biogeochemical processes (Anschutz et al. 2007; Andrieux-Loyer et al. 2008; Wang et al. 2009; Kerr et al. 2010; Cong et al. 2014). The bioavailability of P in aquatic environment influences the primary production rate, species distribution, and ecosystem structure. Monitoring of P content in water and sediment is essential to control and avoid eutrophication of the coastal aquatic environment. Most of the P in the current

natural environment is present in particulate form and is not biologically available, thereby limiting primary production (Yi et al. 2019).

Different forms of P in the sediments can provide valuable information on the origin of P, the degree of pollution from anthropogenic activities, the bioavailability, and also the burial and digenesis of P in sediments (Andrieux and Aminot 1997; Schenau et al. 2000). The sequential extraction method (SEDEX), described in Ruttenberg (1992), has been recognized as a suitable methodology for fractionating different forms of P from sediments. Furthermore, the SEDEX method has high analytical sensitivity and can measure concentrations as low as 0.0005 wt % P, hence suitable for studying marine sediments. This method is the best option for biogeochemical research as it can separate authigenic carbonate fluorapatite from fluorapatite, which is an important distinction as authigenic CFAP represents an oceanic sink for reactive P and detrital FAP does not (Wang et al. 2013). The method separates the sedimentary phosphorus into P adsorbed onto grain surfaces (Ads-P); P associated with easily reducible iron and manganese oxides and/or oxyhydroxides (Fe–P); authigenic P (this includes authigenic carbonate fluorapatite, biogenic apatite, and $CaCO_3$-associated P); detrital P (Det-P); and organic P (OP). Different P phases have different geochemical behaviors, and only certain forms of P (Ads-P, Fe–P, and OP) are bioavailable and released into the water column under various physicochemical processes, such as dissolution, desorption, and reduction. This process depends on the predominant form of P deposited in the sediment layer and its influence on physicochemical characteristics (Ruttenberg 1992; Samadi-Maybodi et al. 2013). However, the method the extraction process is very long and there are chances for partial release of organic phosphorus by CDB reagent (Wang et al. 2013).

The southern part of the Indian Ocean exhibit higher levels of nutrient and other chemical species, primarily due to Indonesian through Flow (ITF) inputs. ITF links the Pacific and Indian Oceans and offers a setup for modifying the stratification within these oceans and sea-air fluxes that impact climatic phenomena such as ENSO and the Asian Monsoon (Potemr 2005). Moreover, the southern part of the Indian Ocean is least investigated regarding nutrient bioavailability/dynamics. It is crucial to gather information on P fraction composition to understand the bioavailability and dynamics of phosphorus in the study area and its influence on marine productivity. This investigation is intended to evaluate the fraction composition, vertical distribution, and bioavailability of phosphorous in core sediments collected from two distinct locations in the Southern Indian Ocean.

Materials and Methods

Study Area

The Indian Ocean has been the least studied compared to the Atlantic and the Pacific Ocean in terms of deep-sea benthic geochemistry. The present investigation was carried out in the Central Indian Ocean Basin (CIOB) under the program "Equatorial Indian Ocean Process-Study Dynamics and Biogeochemistry (EIOPS). Two sediment core samples were collected from this ITF zone. The study area and sampling locations are depicted below (Fig. 1). The second sampling site was a rocky area with manganese nodules. The sampling was very tough at this site, and the length of obtained core was petite with few manganese nodules at the top.

Sampling and Analysis

Sampling was carried out on board from January to February 2010, under the flagship of ORV Sagar Kanya. Sediment samples were collected using a gravity corer (10 cm internal diameter and 10 m long) from the above locations. Total 57 samples for Core I and three samples for Core II were obtained. Samples were kept in a deep freezer at − 20 °C prior to analyses. For chemical fractionation of phosphorus, sediments were firstly sieved through a mesh-size screen of

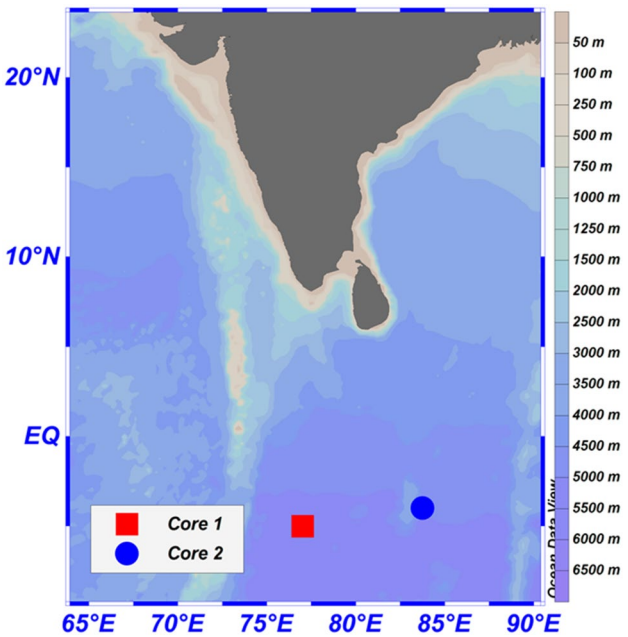

Fig. 1 Sampling sites and location of the investigated area in the Indian Ocean

63 µm, and then 0.5 g freeze dried sediment of each sample in 50 ml extractant was analyzed.

The wet sieving determined the percentage composition of sand, silt, and clay (Krumbein and Pettijohn 1938). Total organic carbon content in sediments was estimated using CHNS Analyzer (Vario EL III CHNS Analyzer) after removing inorganic carbon with 10% HCl (Bouillon et al. 2004). The redox potential of the sediment was measured by the potentiometric method (Radojevic et al.1999). The sedimentary phosphate fractions were separated by the five-step process of the SEDEX method initially devised by Ruttenberg (1992) and later modified by Anderson and Delaney (2000). The fractionation scheme for phosphorous was based on sequential extraction followed by spectrophotometry (Babu and Nath 2005). In Fig. 2, the sequential extraction procedure is displayed in detail, by which phosphorus is classified as different forms of loosely-P, iron-bound P, authigenic-P, detrital-P, and organic-P. In addition, the sediment sample used in a stage was then applied for the next stage. It is worth noting that the extracted solution was filtered through a 0.45 µm GF/C filter membrane before phosphorus measurement, and the pH of the extract was then reached to neutral point (Zhang et al. 2010; Lin et al.2013). In each phase and after extraction, samples were centrifuged at 4000 rpm for 20 min, and phosphorus content was measured according to the method of molybdenum blue/ascorbic acid (Murphy and Riley 1962) at 880 nm wavelength using a UV–Vis spectrophotometer (Genesys 10 UV Thermo Spectronic). Potassium dihydrogen orthophosphate was used as the calibration standard for phosphate estimation. All the containers involved in phosphate determination were cleaned with a nutrient free detergent, rinsed with ultrapure water, soaked in 10% HCl overnight, and rinsed again with ultrapure water (Worsfold et al. 2005). Containers used in the subsampling of sediments (after slicing the core) were twice with the water of interest prior to sample collection. Analytical blanks were employed carefully to nullify the contribution of phosphate from reagents and water involved in the estimation. Analysis was carried out in triplicates to ensure the reproducibility of the data. The vertical distribution graph was plotted using Origin Pro 22. Pearson correlation and Principal Component Analysis were carried out using Origin Pro 22 to assess the relationship between different forms of phosphorus with sediment grain size and total organic carbon (TOC).

Results and Discussion

Distribution of sand, silt, and clay in core sediments is shown in Tables 1 and 2. Texture analysis revealed the dominance of finer particles (silt + clay) throughout the Core. The contents of sand, silt, and clay in Core I and Core II in relation to depth are shown in Figs. 3 and 4, respectively. Sand content varied from 0 to 1.48%, with an average of 0.08%. The maximum content for sand was noticed at a depth range of 90–100 cm. Downcore variation of sand followed a zigzag pattern from the surface to the bottom till it reached

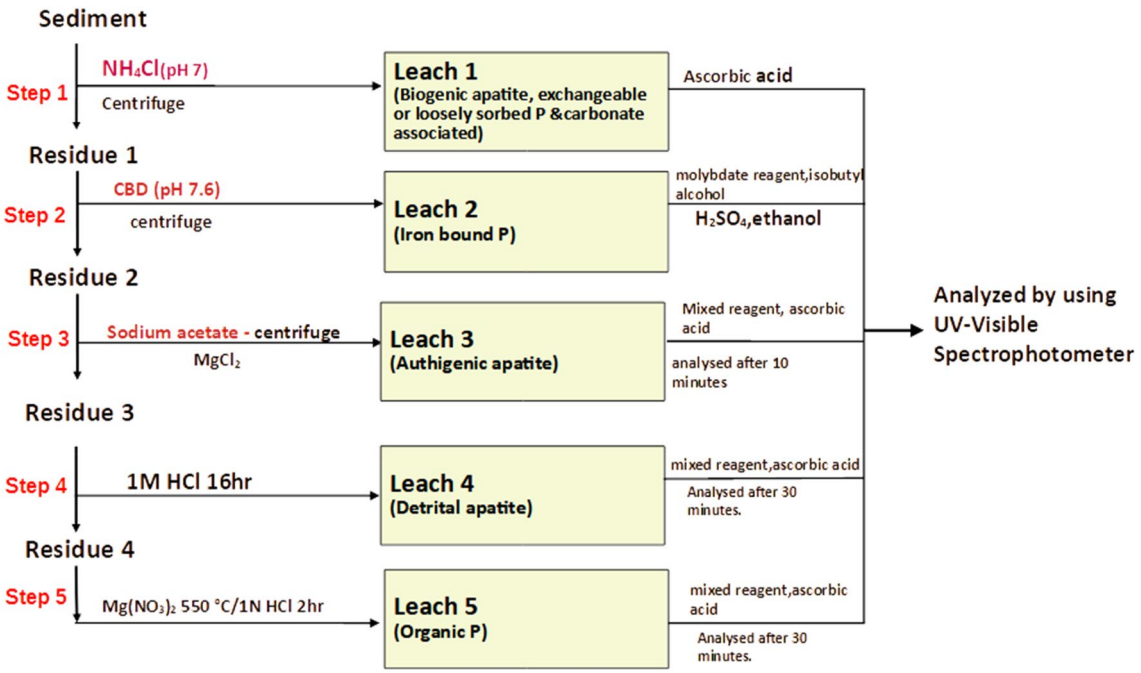

Fig. 2 Sequential extraction of various P fractions

Table 1 Vertical distribution of sand, silt, clay, and TOC in Core I

Depth (cm)	E^h(mV)	Sand (%)	Silt (%)	Clay (%)	TOC (%)
0–10	– 74	0.14 ± 0.02	69.48 ± 3.9	30.37 ± 1.6	0.38 ± 0.02
10–20	– 134	0.58 ± 0.05	83.32 ± 5.62	16.09 ± 2.33	0.89 ± 0.12
20–30	– 163	0.04 ± 0.001	83.23 ± 7.91	16.73 ± 3.85	0.64 ± 0.21
30–40	– 207	0.05 ± 0.025	83.86 ± 11.5	16.09 ± 3.69	0.51 ± 0.19
40–50	– 238	0.30 ± 0.015	71.47 ± 3.25	28.22 ± 6.21	0.26 ± 0.05
50–60	– 231	0.02 ± 0.001	83.05 ± 14.35	16.93 ± 5.77	0.25 ± 0.08
60–70	– 257	0.14 ± 0.10	60.96 ± 6.25	38.89 ± 6.13	0.26 ± 0.10
70–80	– 221	0.10 ± 0.01	82.6 ± 9.85	17.28 ± 1.03	0.25 ± 0.12
80–90	– 248	0.91 ± 0.22	63.37 ± 3.25	35.71 ± 7.08	0.38 ± 0.16
90–100	– 276	1.49 ± 0.5	91.86 ± 15.32	6.65 ± 2.33	0.51 ± 0.16
100–110	– 254	0.11 ± 0.09	92.71 ± 12.22	7.17 ± 1.09	0.38 ± 0.11
110–120	– 313	0.11 ± 0.03	86.02 ± 9.25	13.86 ± 2.55	0.38 ± 0.15
120–130	– 281	0.09 ± 0.02	93.96 ± 6.48	5.94 ± 3.86	0.51 ± 0.22
130–140	– 35	0.04 ± 0.001	92.44 ± 15.36	7.50 ± 1.23	0.38 ± 0.30
140–150	– 37	0.09 ± 0.002	93.48 ± 12.98	6.42 ± 2.32	0.64 ± 0.20
150–160	– 142	0.08 ± 0.004	92.99 ± 10.22	6.93 ± 1.05	0.76 ± 0.31
160–170	– 178	0.09 ± 0.007	93.45 ± 16.02	6.45 ± 2.56	0.63 ± 0.26
170–180	– 18	0.06 ± 0.006	92.71 ± 9.85	7.22 ± 2.81	0.63 ± 0.14
180–190	– 316	0.04 ± 0.011	93.96 ± 13.65	5.99 ± 3.00	0.38 ± 0.22
190–200	– 43	0.07 ± 0.001	93.45 ± 14.09	6.47 ± 1.33	0.38 ± 0.16
200–210	– 142	0.07 ± 0.001	93.32 ± 10.51	6.60 ± 2.06	0.38 ± 0.11
210–220	– 125	0	92.23 ± 16.33	7.77 ± 2.98	0.51 ± 0.23
220–230	– 265	0	81.39 ± 8.10	18.61 ± 2.31	0.38 ± 0.19
230–240	– 133	0	86.00 ± 5.00	14.00 ± 4.00	0.89 ± 0.32
240–250	– 316	0	52.48 ± 9.51	47.52 ± 8.65	0.38 ± 0.18
250–260	– 52	0	55.25 ± 3.02	44.75 ± 12.02	0.76 ± 0.12
260–270	– 56	0	51.23 ± 23.11	48.77 ± 6.05	0.51 ± 0.12
270–280	– 120	0	57.08 ± 3.56	42.92 ± 7.38	0.38 ± 0.6
280–290	– 154	0	65.03 ± 17.61	34.97 ± 13.5	0.51 ± 0.22
290–300	– 28	0	57.93 ± 2.36	42.07 ± 8.34	0.13 ± 0.10
300–310	– 269	0	41.18 ± 10.23	58.82 ± 10.20	0.13 ± 0.03
310–320	– 139	0	35.91 ± 2.53	64.09 ± 15.59	0.13 ± 0.09
320–330	– 82	0	55.08 ± 9.09	44.92 ± 12.65	0.51 ± 0.16
330–340	– 99	0	61.83 ± 9.89	38.17 ± 7.71	0.35 ± 0.12
340–350	– 295	0	57.95 ± 6.79	42.05 ± 2.25	0.38 ± 0.06
350–360	– 65	0	87.03 ± 6.23	12.97 ± 1.03	0.28 ± 0.12
360–370	– 141	0	50.08 ± 3.40	49.92 ± 8.92	0.13 ± 0.04
370–380	– 192	0	92.76 ± 14.2	7.24 ± 1.02	0.13 ± 0.04
380–390	– 251	0	73.47 ± 19.9	26.53 ± 2.31	0.13 ± 0.06
390–400	– 282	0	91.98 ± 6.14	8.02 ± 1.02	0.25 ± 0.10
400–410	– 316	0	77.79 ± 4.51	22.21 ± 2.94	0.38 ± 0.13
410–420	– 334	0	74.35 ± 8.50	25.65 ± 9.21	0.51 ± 0.12
420–430	– 327	0	44.30 ± 6.43	55.70 ± 3.17	0.51 ± 0.10
430–440	– 335	0	42.40 ± 3.42	57.60 ± 3.74	0.38 ± 0.03
440–450	– 341	0	42.77 ± 9.53	57.23 ± 2.69	0.25 ± 0.11
450–460	– 114	0	39.61 ± 1.41	60.39 ± 3.81	0.25 ± 0.12
460–470	– 167	0	47.84 ± 6.43	52.16 ± 2.48	0.13 ± 0.06
470–480	– 254	0	39.49 ± 4.65	60.51 ± 9.56	0.25 ± 0.12
480–490	– 224	0	34.26 ± 1.51	65.74 ± 19.39	0.25 ± 0.11
490–500	– 276	0	27.24 ± 4.00	72.76 ± 5.55	0.25 ± 0.09
500–510	– 209	0	22.37 ± 8.44	77.63 ± 13.46	0.25 ± 0.12

Table 1 (continued)

Depth (cm)	E^h(mV)	Sand (%)	Silt (%)	Clay (%)	TOC (%)
510–520	– 208	0	27.41 ± 8.20	72.59 ± 16.33	0.25 ± 0.10
520–530	– 248	0	38.19 ± 6.75	61.81 ± 36.02	0.38 ± 0.12
530–540	– 228	0	38.30 ± 8.90	61.70 ± 22.11	0.13 ± 0.04
540–550	– 149	0	41.60 ± 9.69	58.40 ± 19.06	0.38 ± 0.20
550–560	– 158	0	47.40 ± 4.50	52.60 ± 14.56	0.13 ± 0.03
560–565	– 214	0	82.89 ± 3.58	17.11 ± 3.07	0.63 ± 0.14

Table 2 Vertical distribution of sand, silt, clay and TOC in core II

Depth	Eh	Sand (%)	Silt (%)	Clay (%)	TOC (%)
0–10	– 257	2.38 ± 0.58	91.77 ± 6.43	5.84 ± 2.02	0.13 ± 0.02
10–20	– 235	7.15 ± 1.21	66.35 ± 8.16	26.49 ± 4.22	0.15 ± 0.01
20–30	– 122	1.89 ± 0.20	71.02 ± 9.51	27.08 ± 3.78	0.13 ± 0.001

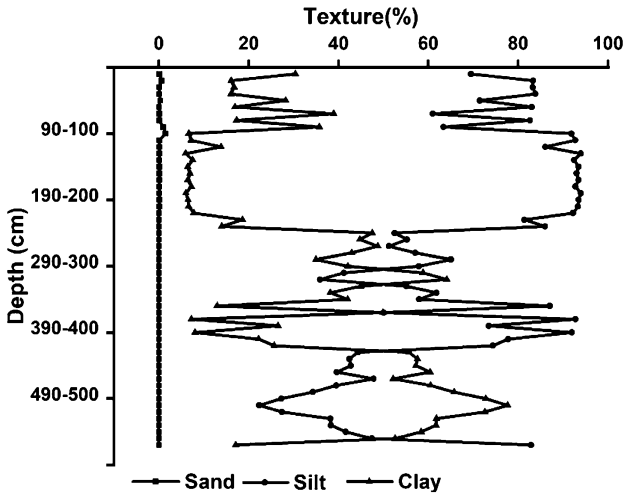

Fig. 3 Vertical variation in grain size of sediments in Core I

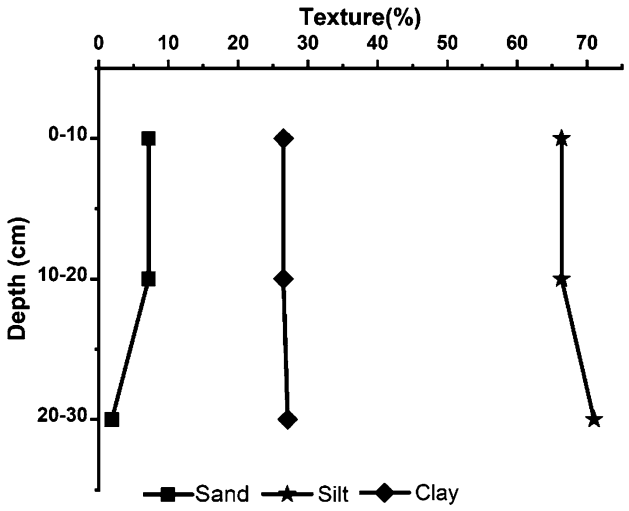

Fig. 4 Vertical distribution of sand, silt, and clay in Core II

100–110 cm (Fig. 3). Sand content was negligible from 210 to 560 cm in depth. Figure 3 depicts a general decline in sand content from surface to bottom. Meanwhile, in core II, the percentage of sand ranged from 2.3 to 7.15 (average: 3.81 ± 0.20%). The highest percentage of sand was recorded at a depth of 10–20 cm. Silt content in core I (Fig. 3) ranged from 22.36 to 93.96% (average: 66.76 ± 1.32%). The maximum silt content was found at a depth of 120–130 cm. The surface of Core I recorded content of 69.48%, increased up to 30–40 cm, and exhibited a steady state, then followed a zigzag pattern. A slight decrease was recorded at 480 to 500–510 cm and slowly increased up to 565 cm. Meanwhile level of silt in Core II (Fig. 4) ranged from 66.35 to 91.77% (average: 76.38 ± 1.76%), and the maximum was observed at the surface. Distribution of clay in Core I is decreased from surface to 30–40 cm of depth; it exhibits a zigzag pattern up to 100–110 cm. Steady state levels of clay were observed at a depth range of 130–220 cm. The highest and lowest clay percentage was recorded in the depth range of 500–510 cm (77.63%) and 120–130 cm (5.94%), respectively. In the case of Core II, an increasing trend for clay level was observed, and it ranged from 5.84 to 27.01% (average: 19.80 ± 0.93%).

From the surface layer till 420 cm of the Core I exhibited a higher silty horizon with a prevalence of fine sediment fraction with both silt and clay silt ranging from 35.91 to 93.96%, whereas the bottom horizon (430–565 cm) was dominated by clay. Core II exhibited dominance of silt. The top horizon (0–10 cm) was enriched with silt (more than 90%), and the subsurface (20–30 cm) was of clayey silt. The Core II exhibited a considerably higher level of sand content compared to Core I, with a variation of 1.89—7.15%. Silt fraction varied from 66.35 to 91.77% and clay 5.84—27.08%. Fine sediments (silt and clay) were the dominant fractions in both the cores in general, which indicated the influence of hydrodynamic conditions. The unique depositional environment helps to trap organic matter. The sediments act as an excellent nutrition reservoir because they are enriched with organic matter. The high nitrogen and phosphorus content associated with organic matter is made available to the overlying water column through various

physico-chemical processes and is utilized by aquatic plants for their growth. Moreover, organic molecules with their ability to make chelate compounds play a significant role in the retention of nutrients in sediments.

Many workers have observed that hypoxic and anoxic conditions facilitate the release of phosphorus from sediments to the water column (Mort et al. 2010). It has been reported that lowering redox potential (E^h) increases the solubility of phosphorus (Ann et al. 2000). Anoxic sediment with low E^h facilitates the reduction of insoluble ferric oxy-hydroxide compounds to soluble ferrous oxy-hydroxide compounds, increasing the sorption sites and thereby resulting in adsorption of a large amount of phosphorus. However, due to low bonding energy, desorption potential is substantially high. In contrast to aerobic sediments, adsorption is relatively less, but retention of phosphorus is more due to high bonding energy (Barik et al.2019).

Information on (TOC) content in sediments is vital to assess the role played by the organic fraction of sediments in the transport, deposition, and retention of metals and nutrients. The distribution of organic carbon in both the core samples is presented above in Tables 1 and 2, and below its variations along the length is shown in Fig. 5 for each Core. In Core I, the maximum TOC content was 0.89 %, and that of the minimum was 0.12% at depth ranges 10–20 cm and 290–300 cm, respectively. In core II, the level of TOC ranged from 0.15 to 0.12% at depth ranges 10–20 cm and 20–30 cm, respectively. Generally, the TOC content was found in sediments with high clay and silt content and lower E^h values. Indeed, organic carbon, buried and conserved in marine sediments, depends on several parameters such as the type of organic matter, terrestrial or marine, as terrestrial is more refractory. Higher TOC content in fine-textured sediments compared to coarse-textured can be ascribed to the fact that differences in C input, rather than long-term decomposition dynamics, since fine-textured sediments tend to be more fertile than coarse-textured due to likely differences in water storage capacity. In an aquatic environment, the content of TOC increases as the texture becomes finer. Clay particles are believed to protect some of the more easily decomposable organic compounds from rapid microbial breakdown through encrustation and entrapment (Rakesh et al. 2020).

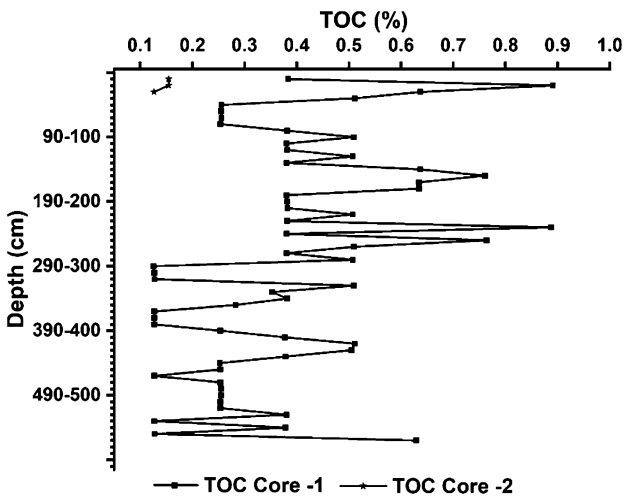

Fig. 5 Vertical distribution of TOC in Core I and core II

Phosphorous Fractions

Sequential extraction provides five phosphorus fractions viz., (1) loosely bound phosphorus (Lo-P) (L1), iron-bound phosphorus (Fe–P) (L2), Authigenic P (P_{auth}) (L3), Detrital (Det-P) (L4) and organic phosphorus (OP) (L5). The values of each phase of P obtained at corresponding depths of each Core are shown in Tables 3 and 4. The fractions of P show a wide range of variations, which are controlled by a number of factors such as the texture of sediments, organic matter content, the intensity of mineralization of organic matter in the sediment, and redox conditions in the sediments.

Loosely bound P Changes in physical, chemical, and biological conditions can induce the release and transformation of phosphorus in the sediments. Variation in the concentration of phosphorus fraction depends on the sources and biogeochemical processes. It may also depend on the rate of sedimentation, post sedimentation changes, tectonics, and the physical and chemical conditions of the depositional basin (Nath et al. 2005). Loosely-P, exchangeable P, or biogenic P (L1) are necessary inorganic phosphorus forms that are adsorbed by sediments, readily released, then enter into the water column above the surface sediment (Yang et al. 2016). From the surface of the Core, there is a distinct change in the trend of Lo-P, which gradually increased to the bottom in the Core I. The bottom layers after 30 cm exhibited relatively higher values for Lo-P (Fig. 6) in Core I. Nevertheless, in Core II, an overall decrease from top to bottom was noticed. The higher concentration may be due to the enhanced input of biogenic components into the sediments after deposition. Schenau et al. (2000) recorded a more remarkable preservation of fish debris at shallower depths (diagenetic process). This might be the reason for higher Lo-P in the deeper layers and other biogenic proxies (sedimentary calcium carbonate). Higher Lo-P may also reflect increased productivity in the area. A reverse trend was noticed in Core II, with higher productivity in the upper layers. During the Holocene and late Pleistocene, which marks the termination of the last glacial age with warmer climates, are more suitable for increased productivity. Higher Lo-P at the top few layers and decreased values at the bottom reflect variations in productivity. An enhanced rate of productivity is usually associated with higher P concentrations. The hydroxyapatite (Ca_{10}

Table 3 Vertical distribution of P fractions (ppm) in Core I

Depth (cm)	L1	L2	L3	L4	L5	Total P	Reactive P	BAP
10	3814.55 ± 43.07	102.23 ± 21.02	764.46 ± 65.23	34.57 ± 16.59	116.34 ± 16.23	4832.15 ± 162.1	4797.59 ± 23.25	4033.13 ± 75.85
20	2319.09 ± 28.92	130.23 ± 23.11	542.89 ± 12.23	18.76 ± 9.12	148.38 ± 19.54	3159.36 ± 40.92	3140.61 ± 96.32	2597.71 ± 57.58
30	5353.57 ± 30.96	78.28 ± 23.55	487.73 ± 10.32	21.32 ± 12.89	83.13 ± 22.46	6024.04 ± 62.18	6002.72 ± 94.56	5514.99 ± 38.31
40	5932.97 ± 34.55	56.23 ± 16.06	294.40 ± 62.43	22.342 ± 9.57	60.53 ± 23.11	6366.48 ± 55.72	6344.14 ± 78.49	6049.73 ± 47.23
50	7628.10 ± 54.52	52.34 ± 14.58	82.466 ± 23.16	16.77 ± 2.03	53.24 ± 10.32	7832.93 ± 64.61	7816.16 ± 46.18	7733.70 ± 56.87
60	5790.14 ± 311.34	40.32 ± 12.11	421.32 ± 36.15	30.23 ± 6.11	41.74 ± 6.24	6323.76 ± 37.95	6293.53 ± 69.26	5872.20 ± 33.69
70	6719.10 ± 83.84	20.23 ± 6.43	120.39 ± 36.42	13.97 ± 3.44	24.18 ± 9.21	6897.89 ± 79.34	6883.92 ± 93.45	6763.52 ± 86.49
80	6751.61 ± 42.04	23.34 ± 8.43	618.66 ± 89.37	26.34 ± 1.25	27.06 ± 3.35	7447.03 ± 52.44	7420.69 ± 70.43	6802.03 ± 44.64
90	5911.27 ± 77.27	98.34 ± 17.84	820.95 ± 96.15	28.44 ± 2.56	100.51 ± 20.51	6959.51 ± 81.83	6931.08 ± 65.61	6110.13 ± 70.84
100	7003.87 ± 44.58	100.34 ± 36.58	620.34 ± 102.54	36.26 ± 9.25	295.53 ± 21.00	8056.35 ± 69.95	8020.09 ± 79.51	7399.75 ± 40.83
150	5353.57 ± 503.84	27.323 ± 9.71	856.57 ± 54.13	32.41 ± 3.55	36.74 ± 3.78	6306.62 ± 75.01	6274.22 ± 56.70	5417.65 ± 51.17
200	4001.12 ± 201.67	90.23 ± 19.80	505.60 ± 24.51	48.23 ± 8.99	104.38 ± 19.52	4749.58 ± 34.49	4701.35 ± 10.12	4195.75 ± 20.18
250	5234.70 ± 217.57	101.23 ± 35.26	805.01 ± 65.24	82.99 ± 9.12	121.06 ± 36.10	6345.00 ± 36.29	6262.01 ± 112.78	5457.00 ± 62.79
300	4573.26 ± 189.84	98.24 ± 10.91	180.22 ± 69.11	63.44 ± 6.58	130.79 ± 22.32	5045.97 ± 98.79	4982.53 ± 54.12	4802.30 ± 28.74
350	5458.43 ± 212.72	84.35 ± 18.35	517.51 ± 84.12	106.33 ± 12.88	92.28 ± 16.24	6258.91 ± 54.31	6152.58 ± 48.12	5635.06 ± 51.84
400	4572.5 ± 256.15	17.32 ± 5.94	345.01 ± 53.24	65.24 ± 12.54	21.23 ± 9.65	5021.30 ± 37.52	4956.06 ± 114.78	4611.06 ± 78.34
450	2669.95 ± 14.65	10.32 ± 6.28	202.29 ± 58.31	74.92 ± 1.36	19.32 ± 6.11	2976.80 ± 22.71	2901.87 ± 27.25	2699.60 ± 48.12
500	3994.23 ± 98.65	9.32 ± 3.22	75.83 ± 12.36	120.90 ± 15.33	15.15 ± 3.46	4215.43 ± 233.02	4094.53 ± 41.35	4018.70 ± 27.44
550	5525.29 ± 43.17	79.32 ± 15.23	868.48 ± 29.00	60.40 ± 2.62	117.93 ± 11.94	6651.44 ± 461.96	6591.04 ± 11.15	5722.55 ± 47.73

Table 4 Vertical distribution of P fractions in Core II (ppm)

Depth (cm)	L1	L2	L3	L4	L5	TP	Reactive P	BAP
10	7015.240 ± 215.10	180.23 ± 12.32	700.12 ± 100.23	87.671 ± 22.56	64.48 ± 15.31	8047.7 ± 65.52	7960.07 ± 43.94	7259.96 ± 52.97
20	1271.295 ± 136.58	147.32 ± 65.73	86.681 ± 16.72	49.319 ± 21.54	45.05 ± 9.65	1599.6 ± 25.22	1550.36 ± 58.00	1463.69 ± 67.77
30	1933.029 ± 210.56	140.32 ± 49.81	29.211 ± 10.34	127.97 ± 13.60	11.39 ± 2.13	2241.9 ± 26.44	2113.95 ± 51.24	2084.70 ± 26.29

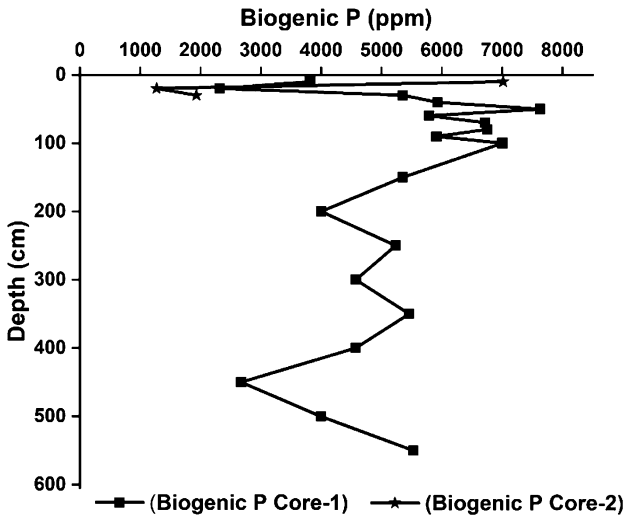

Fig. 6 Variation of Biogenic P (loosely bound P in Core-I and Core-II

$(PO_4)_6(OH)_2)_8$ crystals found in the hard portions of marine fishes are more soluble than fluorapatite. Since the seawater is under saturated with respect to biogenic apatite (Atlas and Pytkowicz 1977), dissolution of fish debris takes place in the upper layer of the sediment (aqueous phase). Exchangeable or loosely sorbed P, carbonate related P, and biogenic P are all included in Leach 1. Figure 6 depicts the variation of this leach with depth. Lo-P in Core I was found to range between 2319.09 and 7628.11 ppm (average: 5189.86 ± 1.67 ppm). A steep downward trend was recorded up to 50 cm, followed by a rise up to 100 cm, a zigzag pattern until 500 cm, and finally an increase at 550 cm. The percentage contribution of Lo-P to TP in Core I (Table 5) ranged from 73.4 to 97.4%, with an average of 88.0%. In the case of Core II, the concentration of L1 was noted to be decreasing. The contribution of Lo-P to TP was from 79.47 to 87.17% (average: 84.29%) in Core II (Table 6).

Easily reducible or reactive iron bound P Variation in concentration of L2 is depicted in Fig. 7. Iron bound P in Core II ranged from 9.32 (0.2% of TP) to 130.23 ppm (4.1% of TP) (average: 64.189 ± 2.32 ppm). However, in the case of Core II, concentration decreases from surface to bottom. The percentage contribution of iron bound P to total P in Core II ranged from 2.24 to 9.21%, with an average of 5.90%. In an alkaline environment, Fe–P can be exchanged for OH^- and other inorganic P molecules that are soluble. Since this kind of phosphorus promotes phytoplankton

Table 5 Percentage contribution of P fraction in core I

Depth(cm)	% contribution of BAP	% contribution of P_{bio}	% contribution of P_{auth}	% contribution of Fe–P	% contribution of Det-P	% contribution of OP
10	83.46	78.94	15.82	2.11	0.71	2.41
20	82.22	73.40	17.18	4.12	0.59	4.69
30	91.55	88.87	8.09	1.30	0.35	1.38
40	95.02	93.19	4.62	0.88	0.35	0.95
50	98.73	97.38	1.05	0.66	0.21	0.68
60	92.86	91.56	6.66	0.63	0.47	0.66
70	98.05	97.41	1.74	0.29	0.20	0.35
80	91.34	90.66	8.31	0.31	0.35	0.36
90	87.80	84.94	11.79	1.41	0.41	1.44
100	91.85	86.94	7.70	1.24	0.45	3.66
150	85.90	84.89	13.58	0.43	0.51	0.58
200	88.34	84.24	10.64	1.90	1.01	2.19
250	86.00	82.50	12.68	1.59	1.38	1.91
300	95.17	90.63	3.57	1.94	1.25	2.59
350	90.03	87.21	8.26	1.34	1.69	1.47
400	91.83	91.06	6.87	0.34	1.29	0.42
450	90.69	89.69	6.79	0.34	2.51	0.64
500	95.33	94.75	1.79	0.22	2.86	0.35
550	86.03	83.06	13.05	1.19	0.91	1.77

Table 6 Percentage contribution of P fraction in core II

Depth(cm)	% contribution of BAP	% contribution of P_{bio}	% contribution of Pauth	% contribution of Fe–P	% contribution of Det-P	% contribution of OP
10	90.21	87.17	8.70	2.24	1.09	0.80
20	91.50	79.47	5.42	9.21	3.08	2.82
30	92.99	86.22	1.30	6.26	5.71	0.51

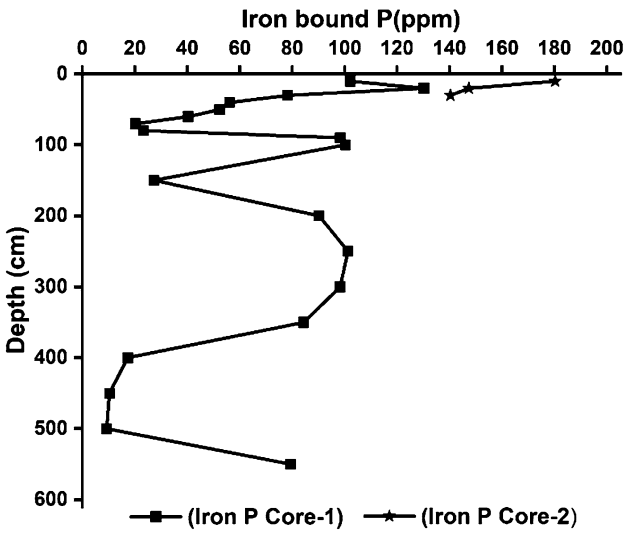

Fig. 7 Variation in Iron bound P in Core I and Core II

growth and development, it may be used to assess their growth (Sundby et al. 1992; Slomp et al. 1996). The environmental conditions influence the concentration of Fe–P. The release of Fe–P into the aqueous phase reduces the pH, and the nutrient fraction is used up by primary producers (Andrieux-Loyer and Aminot 2001; Gurung et al. 2020). P associated with iron oxides has shown a gradual decrease for Core II and an increasing trend in the case of Core I. Initially, the phosphorus is dissolved, and O or OH^- can adsorb it to become a Fe hydroxide (P–O–Fe) or a Fe-oxyhydroxide (P–OH–Fe) form (Mortimer 1941). The low Fe–P at specific depths may therefore be due to the nature of Fe minerals present within sediments (Slomp et al. 1996; Tamburini et al. 2002). In addition to this, under oxidizing conditions, ferric and manganic oxides and hydroxides are important adsorption sites for P (Krom and Berner 1980; Slomp et al. 1996). Ferric and manganic phosphate minerals, such as strengite ($FePO_4.2H_2O$) and trivalent Mn phosphate

($MnPO_3.1.5H_2O$), can form and survive oxidizing conditions. These minerals exist under reduced conditions, resulting in the increased dissolution and release of soluble P into the water (Patrick et al. 1973; Emerson 1976; Emerson and Widmer 1978; Krom and Berner 1980; Moore and Coale 2009). The Core II was taken from the manganese nodule area and also recorded a higher value for Fe–P and TP due to the above reasons. Adsorption of Fe also depends on DO content, and it is seen that there is reduced P sorption at low oxygen conditions. Desorption of P is also greater in acidic conditions. Phosphate buried in sediments will be remobilized later by bacterial degradation. Phosphate present in the pore waters can either be formed by the reductive dissolution of oxides of Fe or by the phosphate released by the degeneration of organic matter (Filipelli and Delaney 1996). However, oxygen depletion and redox potential decrease can stimulate P release from the fraction bound with iron (Kowalczewska-Madura et al. 2019).

Authigenic P Figure 8 depicts the variation in concentration of P_{auth} (L3) in cores I and II. P_{auth} in core-II varied from 29.21 to 700.12 ppm (average: 272.01 ± 3.73 ppm). However, the concentration of L3 in Core II was found to diminish with depth. P_{auth} (Fig. 8) occurred in greater concentrations at the surface of each Core. Percentage contribution of P_{auth} ranged from 1.30 to 8.70% (average: 5.14%) and 1.1 to 17.2% (Average: 8.4%) in Core II (Table 6) and Core I (Table 5), respectively. At the same time, a decrease in both detrital and loosely adsorbed P was also noted, suggesting transformations of phosphate from one phase to another. Most of the remobilized phosphate in the sediment–water interface is removed as authigenic carbonate fluorapatite and does not return to the ocean reservoir (Ruttenberg and Berner 1993; Ingall and Jahnke 1994). Detritus from marine organisms is likely to be the source of P_{auth} (Sekula-Wood et al. 2012). Likewise, conditions with higher and lower oxygen concentrations are favorable for the production of P_{auth}. However, low levels of organic matter and medium oxygen levels limit the formation of this fraction of phosphorus (Kraal et al. 2012; Tsandev et al. 2012). As the Lo-P content is mainly related to productivity and consistent relation between the biogenic and P_{auth} suggests a climatic connection.

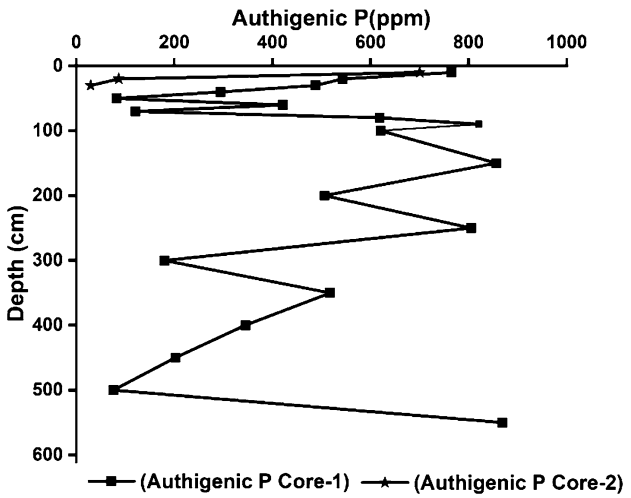

Fig. 8 Variation of P_{auth} with respect to depth in Core I and Core II

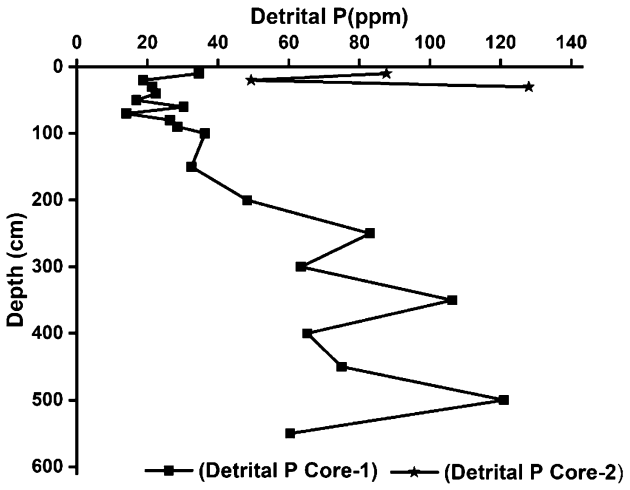

Fig. 9 Variation of Detrital P with respect to depth in Core I and Core II

Detrital P L4 exhibited a zigzag pattern in distribution. The concentration of Det-P (Fig. 9) was lower in both cores. In Core I, it ranged from 13.97 to 120.90 ppm (average: 47.57 ± 3.08 ppm). L4 decreased at the top and increased towards the bottom in Core II. However in Core I, from the surface up to 200 cm, a gradual decrease followed by a

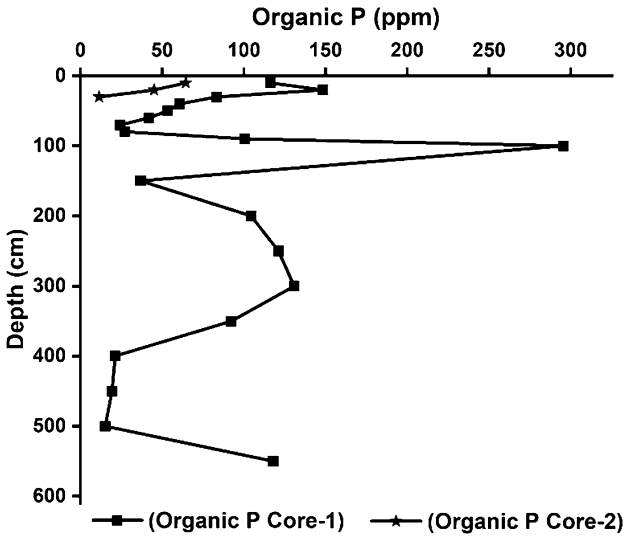

Fig. 10 Variation of Organic P in Core I and Core II

sudden increase was observed (Fig. 10). Det-P contributed 0.2 to 2.9% of total P in Core I (Table 5), with an average of 0.9%. Whereas, in Core II (Table 6), it ranged from 1.08 to 5.7% (average: 3.29%). Det-P is usually derived from weathering of continental rocks. A distinct change at 200 cm suggested a change in provenance type. The difference in P concentration may offer variation in sources with time which can arise due to shifting of the fan limits. The cessation of turbiditic sedimentation due to the abandonment of the active channel may also be a reason for the change in P sources. Essentially two sources, viz., the Himalayan and peninsular Indian and Sri Lankan, can be responsible for a change in detrital P content. Det-P is diagenetically stable, mainly derived from marine sediments and metamorphic rocks (Ruttenberg 1992; Meng et al. 2014). Detrital P has been rarely influenced by biogenic particles due to its mineralogical properties (Ruttenberg 1992) and is therefore recognized as a permanent sink of sediment bound phosphate (Meng et al. 2014).

Organic P There was no particular trend in OP concentration with depth in Core I, even though the upper layers of the Core exhibited a gradual decrease. In contrast, a significant gradual decline was present in Core II (Fig. 10). The concentration of OP ranged from 15.15 to 295.53 ppm (average: 84.71 ± 1.22 ppm) in Core I and from 11.392 to 64.480 ppm (average, 40.31 ± 0.68 ppm) in Core II. OP (Fig. 10) exhibited a decreasing trend with increasing depth in the case of Core II, while no particular trend was observed in Core I. The percentage contribution OP to TP ranged from 0.4 to 4.7% (average, 1.5%) and 0.5 to 2.8% (average: 1.3%) in Core I (Table 5) and Core II (Table 6) respectively. Organic matter in the sediments was susceptible to alteration, and thus the P bound to organic fraction can be converted to other phases. Hence the decline in organic phosphate fraction was due to the biodegradation of OP due to mineralization. The relatively low OP arises due to the increased rate of organic matter decomposition, which releases orthophosphate into pore waters to be captured via Fe oxyhydroxides or authigenic carbonate fluorapatite (Wang et al. 2013). During early diagenesis, the P released from OP degradation is captured through authigenic carbonate fluorapatite formation of oxyhydroxides of Fe or Mn (Filippelli and Delaney 1996; Katsaounos et al. 2007; Hou et al. 2009).

Total Phosphorus (TP) and Reactive P Total concentration of phosphorous in Core I and II are depicted below (Fig. 11). In Core I, TP initially increases and follows a zigzag pattern and then exhibits a decreasing trend with depth. The concentration of TP ranged from 2976.81 to 8056.35 ppm (average: 5866.88 ± 87.32 ppm) in Core I. Concentration of TP in Core II ranged from 1599.68 to 8047.75 ppm (average: 3963.12 ± 56.90 ppm) and exhibited a decreasing trend (Fig. 11). Content of reactant P ranged from 2901.89 to 8020.09 ppm (Average, 5819.30 ± 67.18 ppm) and 1550.36 to 7960.07 ppm in Core I and Core II, respectively (Fig. 12).

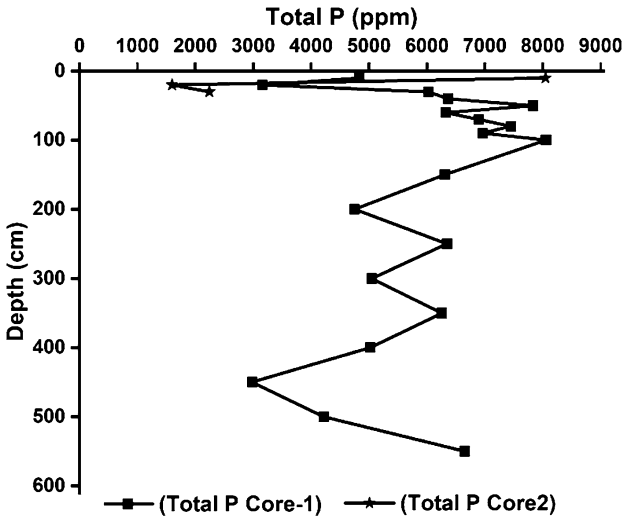

Fig. 11 Vertical distribution of total P in Core I and Core II

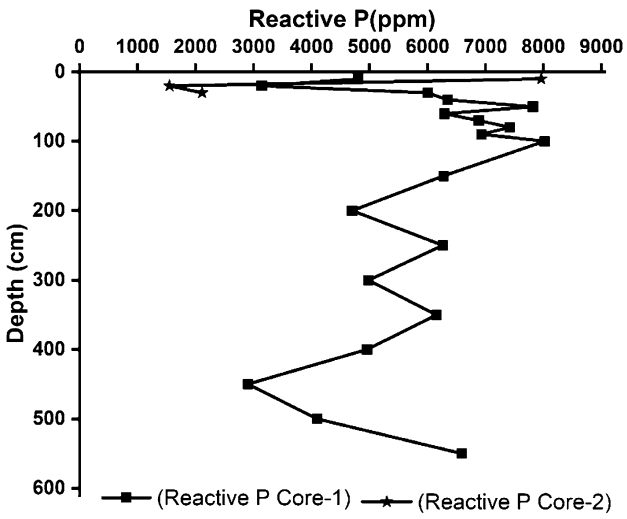

Fig. 12 Vertical distribution of reactive P in Core I and Core II

Statistical Analysis

Principal component analysis was used to identify and interpret the relations among phosphorus types, grain size, and TOC. When we analyzed core I, total variance explained by PC1 and PC2 (Fig. 13) was 63.41%, with PC1 accounting for 41.41% and PC2 accounting for 22.37% of the total variance. Lo-P was positively correlated with sand ($r = 0.26$) and silt ($r = 0.20$) (Fig. 13). P_{auth} was positively correlated with silt ($r = 0.21$), sand ($r = 0.24$), and TOC ($r = 0.43$). Positive relation between TOC with P_{auth} implies the remarkable role of TOC in dispersion of this class of phosphorus

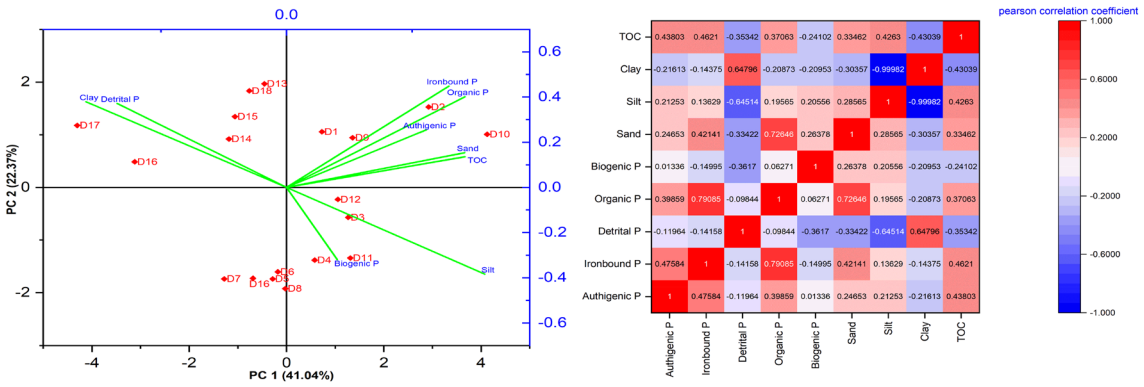

Fig. 13 Principal Component Analysis and Pearson correlation matrix (Heat map) for Core I

(Łukawska-Matuszewska and Bolałek, 2008). Similarly, OP correlated positively with silt ($r=0.19$), sand ($r=0.27$), and TOC ($r=0.37$). Fe–P is also positively linked with silt in good agreement with the observations of Stone and English (1993). A significant positive correlation exists between the Fe–P and TOC ($r=0.46$ $p=0.046$) (Fig. 13), implying that TOC is an important factor in the concentration and distribution of the P species in the sediments. Fe–P significantly correlated with the P_{auth} ($r=0.47$, $p<0.05$) and OP ($r=0.79$, $p<0.02$) similar to other investigations (Mao et al. 2021; Souza et al. 2022). Det-P was mostly concentrated in clay ($r=0.64$, $p<0.02$), comparable with the observations of Yang et al. 2016, who suggested that Det-P is probably associated with the transport of terrigenous material.

In the case of Core II, the total variance explained by PC1 and PC2 (Fig. 14) was 100%, with PC1 accounting for 66.33% and PC2 accounting for 33.67% of the total variance. Lo-P positively correlated with silt (r = 0.99). It could be due to the larger surface area of the finer particles providing a higher adsorption area for phosphate (Wang et al. 2006; Barik et al. 2019). P_{auth} positively correlated with silt ($r=0.96$). Iron bound P also exhibited a similar correlation to Lo-P and P_{auth}. Meanwhile OP correlated positively with the silt ($r=0.65$), and TOC ($r=0.18$).

Assessment of Bioavailability of Phosphorous

It is crucial to identify the potential bioavailable P in surface sediments because BAP can provide information on eutrophication or offset P limitation (Andrieux and Aminot 1997; Yang et al. 2016; Li et al. 2018). BAP refers to the sum of immediately available phosphorus and potential phosphorus that can be transformed into a functional form by biogeochemical process (Sonzogni et al. 1982; Wang et al. 2009). Bioavailable P includes Ex-P, Fe–P, and OP (Kang et al. 2017; Bastami et al. 2018; Loh et al. 2020; Gu et al. 2021). BAP is the upper limit of phosphorus in the sediments; it can be released into the overlying water column with changing environmental conditions (Meng et al. 2014; Kang et al. 2017; Wang et al. 2017). When sedimentary BAP is released to the overlying waters, the primary productivity in the water body will be enhanced (Coelho et al. 2004; Hou et al. 2009; Kang et al. 2017). Remineralization of OP enhances phosphorus bioavailability (Colman et al. 2005; Joshi et al. 2015). Loosely bound phosphate is the most labile P form

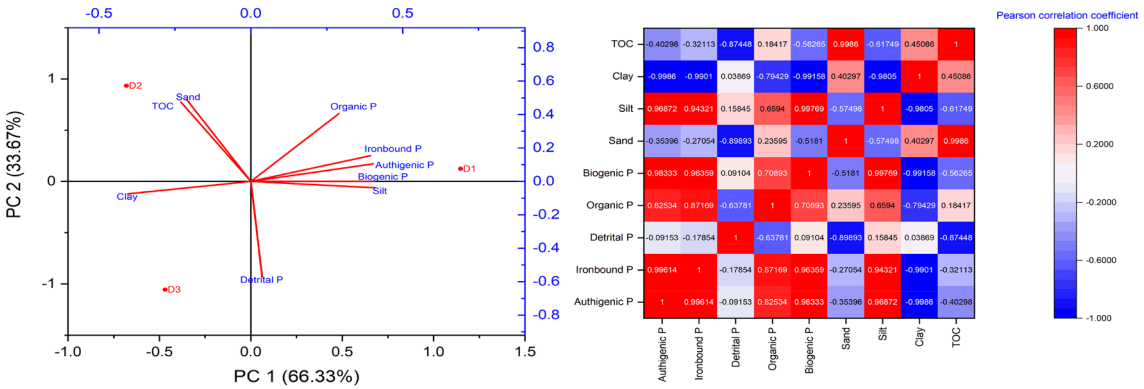

Fig. 14 Principal Component Analysis and Pearson correlation matrix (Heat map) for Core II

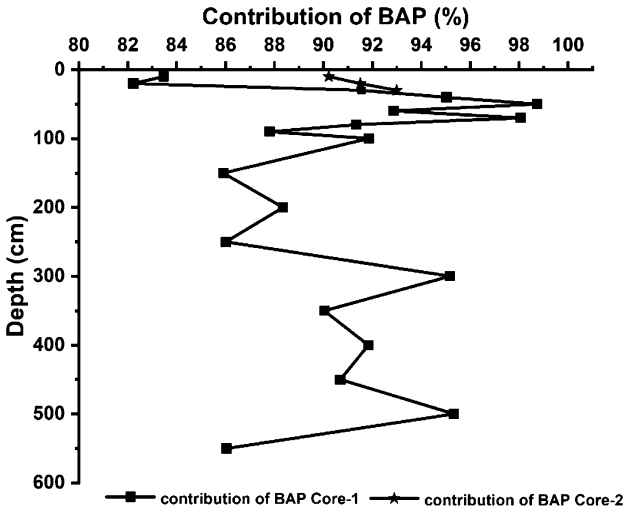

Fig. 15 Contribution of BAP to total phosphorous

because it is loosely sorbed, exchangeable, and water soluble. Fe–P is pH and redox-sensitive, and during anoxic conditions, it serves as a source of internal phosphate loading. During aerobic organic matter decomposition, OP is released as phosphate. The released phosphorus is available for algal growth and can further sustain the eutrophication processes (Coelho et al. 2004). Sedimentary OP can transform into Ex-P and/or Fe–P and Ca–P when environmental conditions change (Joshi et al. 2015; Kang et al. 2017). Organic matter containing phosphate decomposes and transform into inorganic form under situations like low sediment deposition and oxic condition (Colman et al. 2005; Paytan and McLaughlin 2007; Mort et al. 2010; Asmala et al. 2017). The contribution of BAP to total P content in Core I ranged from 82.2 to 98.7% (average: 90.6%) (Fig. 15). In the case of Core II, BAP accounted for 90.2 to 93.0% of total P (average: 91.6%). The high BAP content in the core samples implied the fact that the sediments in the study area act as a sink for phosphorous, and the changing environmental conditions can trigger the release of phosphate to the overlying water column leading to eutrophication.

Conclusion

Texture compositions in Core I and II were dominated by fine-grained sediments. Phosphorous fractionation revealed the fact that > 80% of sedimentary phosphorus in the study area was composed of Lo-P. P_{auth} was perceived as an abundant phosphorus fraction in the study area. Statistical analysis revealed that phosphorous fractions correlated positively with the silt, clay, and TOC. Positive correlations of silt with all P fractions (except Det-P) suggested the role of adsorption on fine grained sediments facilitating the accumulation of phosphorous forms in both cores. The interrelationships among Fe–P, $P_{auth,}$ and OP suggested similar sources and patterns of behavior. The phosphate fraction composition in core I followed the trend: loosely bound > authigenic > organic phosphorous > iron bound > detrital. Whereas in core II loosely bound > authigenic > iron bound > detrital > organic phosphorous. Phosphorus is a limiting component for oceanic productivity, and its concentration was influenced not only by continental weathering but also by the physical, chemical, and biological processes in the Ocean at the time of sediment deposition, as well as post-depositional diagenetic changes. The enhanced bioavailable phosphate levels in the core sediments implied the role of sediments to act as a sink for phosphate, and the drastic alteration in environmental conditions can trigger the nutrient release to the water column and subsequent eutrophication.

Acknowledgements The authors are thankful to Dr. Prasannakumar S, Scientist, CSIR-National Institute of Oceanography, Goa, for giving the opportunity to participate in the O.R.V Sagarkanya SK-267 voyage. The support from the Department of Chemical Oceanography, Cochin University of Science and Technology is acknowledged.

Funding Open Access funding provided by the Qatar National Library.

References

Abu-Hmeidan HY, Williams GP, Miller AW (2018) Characterizing total phosphorus in current and Geologic Utah Lake sediments: implications for water quality management issues. Hydrology 5:8. https://doi.org/10.3390/hydrology5010008

Anderson LD, Delaney ML (2000) Sequential extraction and analysis of phosphorus in marine sediments: streamlining of the SEDEX procedure. Limnol Oceanogr 45:509–515. https://doi.org/10.4319/lo.2000.45.2.0509

Andrieux F, Aminot A (1997) A two-year survey of P speciation in the sediments of Bay of Seine (France). Cont Shelf Res 17:1229–1245. https://doi.org/10.1016/S0278-4343(99)00003-5

Andrieux-Loyer F, Aminot A (2001) Phosphorus forms related to sediment grain size and geochemical characteristics in French coastal areas. Estuar Coast Shelf Sci 52:617–629. https://doi.org/10.1006/ecss.2001.0766

Andrieux-Loyer F, Philippon X, Bally G et al (2008) Phosphorus dynamics and bioavailability in sediments of the Penze Estuary (NW France): In: relation to annual ´ P-fluxes and occurrences of

Alexandrium minutum. Biogeochemistry 88:213–231. https://doi.org/10.1007/s10533-008-9199-2
Ann Y, Reddy KR, Delfino JJ (2000) Influence of redox potential on phosphorus solubility in chemically amended wetland organic soils. Ecol Eng 14:169–180. https://doi.org/10.1016/S0925-8574(99)00027-0
Anschutz P, Chaillou G, Lecroart P (2007) Phosphorus diagenesis in sediment of the Thau Lagoon. Estuar Coast Shelf Sci 72:447–456. https://doi.org/10.1016/j.ecss.2006.11.012
Asmala E, Carstensen J, Conley DJ et al (2017) Efficiency of the coastal filter: nitrogen and phosphorus removal in the Baltic Sea. Limnol Oceanogr 62:S222–S238. https://doi.org/10.1002/lno.10644
Atlas E, Pytkowicz M (1977) Solubility behaviour of apatites in seawater. Limnol Oceanogr 22:290–300. https://doi.org/10.4319/lo.1977.22.2.0290
Bagalwa M (2021) Relationship between Atmospheric Deposition of Nutrient (N and P) Concentration and Wind Direction in Lake Kivu Watershed, DR Congo Side. Sch Acad J Biosci 12:395–404. https://doi.org/10.36347/sajb.2021.v09i12.003
Barik SK, Bramha S, Bastia TK et al (2019) Characteristics of geochemical fractions of phosphorus and its bioavailability in sediments of a largest brackish water lake, South Asia. Ecohydrol Hydrobiol 19:370–382. https://doi.org/10.1016/j.ecohyd.2019.02.002
Bastami KD, Neyestani MR, Raeisi H et al (2018) Bioavailability and geochemical speciation of phosphorus in surface sediments of the Southern Caspian Sea. Mar Pollut Bull 126:51–57. https://doi.org/10.1016/j.marpolbul.2017.10
Benitez-Nelson CR (2000) The biogeochemical cycling of phosphorus in marine systems. Earth Sci Rev 51:109–135. https://doi.org/10.1016/S0012-8252(00)00018-0
Bouillon S, Moens T et al (2004) Resource utilization patterns of epifauna from mangrove forests with contrasting inputs of local versus imported organic matter. Mar Ecol Prog Ser 278:77–88. https://doi.org/10.3354/meps278077
Brady NC (1995) The nature and properties of soils, 10th edn. Prentic Hall of India Private Ltd, New Delhi, p 621
Coelho JP, Flindt MR, Jensen HS et al (2004) Phosphorus speciation and availability in intertidal sediments of a temperate estuary: relation to eutrophication and annual P-fluxes. Estuar Coast Shelf Sci 61:583–590. https://doi.org/10.1016/j.ecss.2004.07.001
Colman AS, Blake RE, Karl DM et al (2005) Marine phosphate oxygen isotopes and organic matter remineralization in the oceans. Proc Natl Acad Sci 102:13023–13028. https://doi.org/10.1073/pnas.0506455102
Cong M, Jian T, Y-zao Qi et al (2014) Phosphorus forms and distribution in Zhejiang coastal sediment in the East China Sea. Int J Sediment Res 29:278–284. https://doi.org/10.1016/S1001-6279(14)60043-3
Dan SF, Liu SM, Yang B (2020) Geochemical fractionation, potential bioavailability and ecological risk of phosphorus in surface sediments of the Cross River Estuary system and adjacent shelf, South East Nigeria (West Africa). J Mar Syst 201:103244. https://doi.org/10.1016/j.jmarsys.2019.103244
Delaney ML (1998) Phosphorus accumulation in marine sediments and the oceanic phosphorus cycle. Glob Biogeochem Cycles 12:563–572. https://doi.org/10.1029/98GB02263
Emerson S (1976) Early diagenesis in anaerobic lake sediments: chemical equilibria in interstitial waters. Geochim Cosmochim Acta 40:925–934. https://doi.org/10.1016/0016-7037(76)90141-1
Emerson S, Widmer G (1978) Early diagenesis in anaerobic lake sediments-II. Thermodynamic and kinetic factors controlling the formation of iron phosphate. Geochim Cosmochim Acta 42:1307–1316. https://doi.org/10.1016/0016-7037(78)90035-2
Filipelli GM, Delaney ML (1996) Phosphorus geochemistry of equatorial Pacific sediments. Geochira Cosmochim Acta 60:1479–1495. https://doi.org/10.1016/0016-7037(96)00042-7
Gu YG, Wang Y, Ouyang J et al (2021) Impacts of coastal aquaculture on sedimentary phosphorus speciation and fate: evidence from a seaweed cultivation area off Nan'ao Island, South China. Mar Pollut Bull 171:112719. https://doi.org/10.1016/j.marpolbul.2021.112719
Gurung DP, Chen N, Waguespack Y et al (2020) Phosphorus speciation and bioavailability in the surface sediments of Maryland Coastal Bays. J Coast Res 36:1266–1277. https://doi.org/10.2112/JCOASTRES-D-19-00131.1
Hou LJ, Liu M, Yang Y et al (2009) Phosphorus speciation and availability in intertidal sediments of the Yangtze Estuary, China. Appl Geochem 24:120–128. https://doi.org/10.1016/j.apgeochem.2008.11.008
Ingall E, Jahnke R (1994) Evidence for enhanced phosphorus regeneration from marine sediments overlain by oxygen depleted waters. Geochim Cosmochim Acta 58:2571–2575. https://doi.org/10.1016/0016-7037(94)90033-7
Jahnke RJ (1992) The phosphorus cycle. In: Butcher SS, Charlson RJ, Orians GH, Wolfe GV (eds) Global biogeochem cyc. Academic Press, New York
Jiang S, Lu H, Liu J et al (2018) Influence of seasonal variation and anthropogenic activity on phosphorus cycling and retention in mangrove sediments: a case study in China. Estuar Coast Shelf Sci 202:134–144. https://doi.org/10.1016/j.ecss.2017.12.011
Joshi SR, Kukkadapu RK, Burdige DJ et al (2015) Organic matter remineralization predominates phosphorus cycling in the mid-bay sediments in the Chesapeake Bay. Environ Sci Technol 49:5887–5896. https://doi.org/10.1021/es5059617
Kang X, Song J, Yuan H et al (2017) Phosphorus speciation and its bioavailability in sediments of the Jiaozhou Bay. Estuar Coast Shelf Sci 188:127–136. https://doi.org/10.1016/j.ecss.2017.02.029
Katsaounos CZ, Giokas DL, Leonardos ID, Karayannis MI (2007) Speciation of phosphorus fractionation in river sediments by explanatory data analysis. Water Res 41:406–418. https://doi.org/10.1016/j.watres.2006.10.028
Kerr JG, Burford M, Olley J, Udy J (2010) The effects of drying on phosphorus sorption and speciation in subtropical river sediments. Mar Freshwater Res 61:928–935. https://doi.org/10.1071/MF09124
Kowalczewska-Madura K, Kozak A, Dera M, Gołdyn R (2019) Internal loading of phosphorus from bottom sediments of two mesoeutrophic lakes. Int J Environ Res 13:235–251. https://doi.org/10.1007/s41742-019-00167-y
Kraal P, Slomp CP, Reed DC, Reichart GJ, Poulton SW (2012) Sedimentary phosphorus and iron cycling in and below the oxygen minimum zone of the northern Arabian Sea. Biogeosciences 9:2603–2624. https://doi.org/10.5194/bg-9-2603-2012
Krom MD, Berner RA (1980) Adsorption of phosphate in anoxic marine sediments 1. Limnol Oceanogr 25:797–806. https://doi.org/10.4319/lo.1980.25.5.0797
Krumbein WC, Pettijohn FJ (1938) Manual of sedimentary petrography. Appleton-Century-Crofts, New York
Leote C, Mulder L, Epping E (2014) A budget of bioavailable inorganic phosphorus in the sediment for the western Wadden Sea. J Sea Res 87:79–90. https://doi.org/10.1016/j.seares.2013.12.009
Li H, He H, Yang S et al (2018) The contribution of opal-associated phosphorus to bioavailable phosphorus in surface and core sediments in the East China Sea. J Ocean Univ China 17:571–580. https://doi.org/10.1007/s11802-018-3387-z
Lin P, Guo L, Chen M, Cai Y (2013) Distribution, partitioning and mixing behavior of phosphorus species in the Jiulong River estuary. Mar Chem 157:93–105. https://doi.org/10.1016/j.marchem.2013.09.002
Loh PS, Ying CY, Alnoor HIM et al (2020) Comparative study on the elucidation of sedimentary phosphorus species using two methods, the SMT and SEDEX methods. J Anal Methods Chem. https://doi.org/10.1155/2020/8548126

Łukawska-Matuszewska K, Bolałek J (2008) Spatial distribution of phosphorus forms in sediments in the Gulf of Gdańsk (southern Baltic Sea). Cont Shelf Res 28:977–990. https://doi.org/10.1016/j.csr.2008.01.009

Mao C, Li T, Rao W et al (2021) Chemical speciation of phosphorus in surface sediments from the Jiangsu Coast, East China: Influences, provenances and bioavailabilities. Mar Pollut Bull 163:111961. https://doi.org/10.1016/j.marpolbul.2020.111961

Maslukah L, Wirasatriya A, Yusuf M et al (2021) Phosphorous fractionation distribution in surface sediments of the Jobokuto Bay. Molekul 16:100–109. https://doi.org/10.20884/1.jm.2021.16.2.572

Meng J, Yao P, Yu Z et al (2014) Speciation, bioavailability and preservation of phosphorus in surface sediments of the Changjiang estuary and adjacent East China Sea inner shelf, Estuar Coast. Shelf Sci 144:27–38. https://doi.org/10.1016/j.ecss.2014.04.015

Moore P, Coale F (2009) Phosphorus fractionation in flooded soils and sediments. In: Methods of phosphorus analysis for soils, sediments, residuals, and waters, 2nd edn, vol 408. Southern Coop Series Bull, pp 61–70.

Mort HP, Slomp CP, Gustafsson BG, Andersen TJ (2010a) Phosphorus recycling and burial in Baltic Sea sediments with contrasting redox conditions. Geochim Cosmochim Acta 74:1350–1362. https://doi.org/10.1016/j.gca.2009.11.016

Mortimer CH (1941) The exchange of dissolved substances between mud and water in lakes. J Ecol 29:280–329. https://doi.org/10.2307/2256395

Murphy J, Riley JP (1962) A modified single solution method for the determination of phosphate in natural waters. Anal Chim Acta 27:31–36. https://doi.org/10.1016/S0003-2670(00)88444-5

Nath BN, Nabar S, Ingole BS, Khadge NH, Valsangkar AB, Srinivas K, Raghukumar C (2005)Geochemical changes induced by benthic disturbance experiment in the Central Indian Basin: Organic Carbon Dynamics. Appl Geochem

Patrick WH, Gotoh S, Williams BG (1973) Strengite dissolution in flooded soils and sediments. Science 179:564–565. https://doi.org/10.1126/science.179.4073.564

Paytan A, McLaughlin K (2007) The oceanic phosphorus cycle. Chem Rev 107:563–576. https://doi.org/10.1021/cr0503613

Potemr JT (2005) Indonesian throughflow transport variability estimated from satellite altimetry. Oceanogr 18(4)

Radojevic M, Bashkin V, Bashkin VN (1999) Practical environmental analysis. Royal Society of Chemistry

Rakesh S, Sinha AK, Mukhopadhyay P (2020) Vertical distribution of TOC, TN and other important soil attributes and their relationship in Alfisol and Entisol of West Bengal. Int J Environ Clim Change. https://doi.org/10.9734/ijecc/2020/v10i130176

Reddy KR, Wetzel RG, Kadlec RH (2005) Biogeochemistry of phosphorus in wetlands. Phosphorus Agric Environ 46:263–316. https://doi.org/10.2134/agronmonogr46.c9

Ruttenberg KC (1992) Development of a sequential extraction method for different forms of phosphorus in marine sediments. Limnol Oceanogr 37:1460–1482. https://doi.org/10.4319/lo.1992.37.7.1460

Ruttenberg KC (2003) The global phosphorus cycle. Treatise Geochem. https://doi.org/10.1016/b0-08-043751-6/08153-6

Ruttenberg KC, Berner RA (1993) Authigenic apatite formation and burial in sediments from non-upwelling, continental margin environments. Geochim Cosmochim Acta 57:991–1007. https://doi.org/10.1016/0016-7037(93)90035-U

Schenau SJ, Slomp CP, De Lange GJ (2000) Phosphogenesis and active phosphorite formation in sediments from the Arabian Sea oxygen minimum zone. Mar Geol 169:1–20. https://doi.org/10.1016/S0025-3227(00)00083-9

Sekula-Wood E, Benitez-Nelson CR, Bennett MA, Thunell R (2012) Magnitude and composition of sinking particulate phosphorus fluxes in Santa Barbara Basin, California. Glob Biogeochem Cycles. 15:10. https://doi.org/10.1029/2011gb004180

Serna J, Bergwitz C (2020) Importance of dietary phosphorus for bone metabolism and healthy aging. Nutrients. https://doi.org/10.3390/nu12103001

Slomp CP, Van der Gaast SJ, Van Raaphorst W (1996) Phosphorus binding by poorly crystalline iron oxides in North Sea sediments. Mar Chem 52:55–73. https://doi.org/10.1016/0304-4203(95)00078-X

Sonzogni WC, Chapra SC, Armstrong DE (1982) Bioavailability of phosphorus inputs to lakes. J Environ Qual 11:555–563. https://doi.org/10.2134/jeq1982.00472425001100040001x

Souza GK, Kuroshima KN, Abreu JG, Manzoni GC (2022) Speciation and distribution of sedimentary phosphorus in an important mariculture area, armação do Itapocoroy Bay, Southern Brazil. Reg Stud Mar Sci 49:102137. https://doi.org/10.1016/j.rsma.2021.102137

Stone M, English MC (1993) Geochemical composition, phosphorus speciation and mass transport of fine-grained sediment in two Lake Erie tributaries. In: Proceedings of the Third International Workshop on Phosphorus in Sediments, pp 17–29. https://doi.org/10.1007/978-94-011-1598-8_2

Sundby B, Gobeil C, Silverberg N, Alfonso M (1992) The phosphorus cycle in coastal marine sediments. Limnol Oceanogr 37:1129–1145. https://doi.org/10.1007/978-94-011-1598-8_37

Tamburini C, Garcin J, Ragot M, Bianchi A (2002) Biopolymer hydrolysis and bacterial production under ambient hydrostatic pressure through a 2000 m water column in the NW Mediterranean. Deep Sea Res Part II 49:2109–2123. https://doi.org/10.1016/S0967-0645(02)00030-9

Tsandev I, Reed DC, Slomp CP (2012) Phosphorus diagenesis in deep-sea sediments: sensitivity to water column conditions and global scale implications. Chem Geol 330–331:127–139. https://doi.org/10.1016/j.chemgeo.2012.08.012

Tyrrell T (1999) The relative influences of nitrogen and phosphorus on oceanic primary production. Nature 400:525–531. https://doi.org/10.1038/22941

Wang XJ, Xia SQ, Chen L, Zhao JF, Renault NJ, Covelo JM (2006) Nutrients removal from municipal wastewater by chemical precipitation in a moving bed biofilm reactor. Process Biochem J 41:824–828. https://doi.org/10.1016/j.procbio.2005.10.015

Wang P, He M, Lin C, Men B, Liu R, Quan X, Yang Z (2009) Phosphorus distribution in the estuarine sediments of the Daliao river, China. Estuar Coast Shelf Sci 84:246–252. https://doi.org/10.1016/j.ecss.2009.06.020

Wang C, Zhang Y, Li H, Morrison RJ (2013) Sequential extraction procedures for the determination of phosphorus forms in sediment. Limnol 14:147–157. https://doi.org/10.1007/s10201-012-0397-1

Wang Q, Han K, Wang J, Gao J, Lu C (2017) Influence of phosphorous based additives on ash melting characteristics during combustion of biomass briquette fuel. Renew Energy 113:428–437. https://doi.org/10.1016/j.renene.2017.06.018

Worsfold PJ, Gimbert LJ, Mankasingh U et al (2005) Sampling, sample treatment and quality assurance issues for the determination of phosphorus species in natural waters and soils. Talanta 66:273–293. https://doi.org/10.1016/j.talanta.2004.09.006

Yang B, Liu SM, Wu Y, Zhang J (2016) Phosphorus speciation and availability in sediments off the eastern coast of Hainan Island, South China Sea. Cont Shelf Res 118:111–127. https://doi.org/10.1016/j.csr.2016.03.003

Yi Z, Yang Y, Yan C et al (2019) The influence of periphyton biofilm on phosphorus migration in sediments. Int J Environ Res 13:327–335. https://doi.org/10.1007/s41742-019-00182-z

Zhang JZ, Guo L, Fischer CJ (2010) Abundance and chemical speciation of phosphorus in sediments of the Mackenzie River Delta, the Chukchi Sea and the Bering Sea: importance of detrital apatite. Aquat Geochem 16:353–371. https://doi.org/10.1007/s10498-009-9081-4